A Partially-planarised Hole-transporting Quart-*p*-phenylene for Perovskite Solar Cells

Juan P. Mora-Fuentes,[a] Diego Cortizo-Lacalle,[a] Silvia Collavini,[a] Karol Strutyński,[b] Wolfgang R. Tress,[c] Michael Saliba,[c] Shaik M. Zakeeruddin,[c] Ivet Kosta,[d] Manuel Melle-Franco,[b] Michael Grätzel,[c]* Juan Luis Delgado,[a,e]* Aurelio Mateo-Alonso[a,e]*

[a] *POLYMAT, University of Basque Country UPV-EHU, Avenida Tolosa 72, E-20018 Donostia-San Sebastián, Spain.*

[b] *CICECO-Aveiro Institute of Materials, Department of Chemistry, 3810-193, Aveiro, Portugal.*

[c] *Laboratory for Photonics and Interfaces, Institute of Chemical Sciences and Engineering, École Polytechnique Fédérale de Lausanne, CH-1015 Lausanne, Switzerland*

[d] *CIDETEC, Paseo Miramón, 191. E-20014 Donostia-San Sebastián, Spain.*

[e] *Ikerbasque, Basque Foundation for Science, Bilbao, Spain.*

Abstract

Herein, we describe the synthesis of a hole transporting material based on a partially planarised quart-p-phenylene core incorporating tetraketal and diphenylamine substituents that show optimal energy levels and solubility for perovskite solar cell applications. Triple-cation perovskite devices incorporating such quart-p-phenylene derivative show power-conversion efficiencies, short circuit currents, open circuit voltages, and fill factors that are comparable to those of spiro-OMeTAD.

In recent years, perovskite solar cells (PSCs) have rapidly emerged as a promising technology in photovoltaics.[1-10] Current state-of-the-art PSCs have surpassed the power-conversion efficiencies (PCEs) of organic solar cells[11-14] and dye-sensitized solar cells,[2, 15-17] and recently surpassed those reached with the current market leader polycrystalline silicon.[18-21] In PSCs, light is harvested by organic-inorganic metal halide perovskites, which show strong absorption in the UV-visible-near infrared range, large free charges diffusion lengths, small exciton binding energy, and low-cost fabrication. The free charges formed in the perovskite after the absorption of light are separated in electrons and holes, which are respectively transported to the electrodes by an electron transporting material (ETM) and a hole transporting material (HTM) to close the circuit.[8, 22, 23]

Currently, the most commonly used small molecule as HTM is 2,2′,7,7′-tetrakis(*N,N*-bis(*p*-methoxyphenyl)amino)-9,9′-spirobifluorene[20] (*spiro*-OMeTAD) (Figure 1). However, the long synthetic route of *spiro*-OMeTAD limits its suitability for large-scale industrial applications. Furthermore, the exploration of other HTM provides key and valuable information for the design of new materials with improved processability and performance for PSCs. *Spiro*-OMeTAD is constituted by two fluorene units in a spiro configuration with two triphenylamines at the 2 and 7 positions. Its electronic structure is analogous to that of a planarised *p*-biphenylene. Oligo- and poly-*p*-phenylenes[24, 25] are a class of conjugated materials that have received much interest as hole transporting materials,[26-31] since the HOMO level can be controlled with the number of rings in the *p*-phenylene chain.[24, 25] Nevertheless, the phenylene rings adopt a non-planar conformation with a dihedral angle that (i) partially interrupts the longitudinal conjugation resulting in a lower effective conjugation, and also (ii)

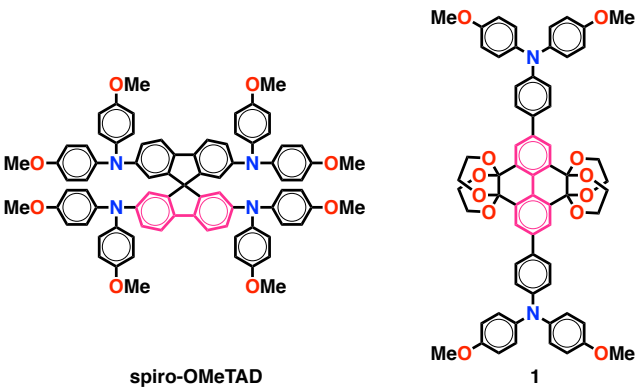

Figure 1. Structure of *spiro*-OMeTAD and of quart-*p*-phenylene **1**

interferes with the co-facial packing optimal for charge transport. Therefore, planarised *p*-phenylenes with a higher effective conjugation are attractive candidates for the design of efficient HTM.

Herein, we report the synthesis and characterisation of a novel HTM based on a partially planarised quart-*p*-phenylene structure (**1**), in which the two central rings are embedded on a planar tetrahydropyrene core with four lateral tetraketals (Figure 1) that enhance the stability of the tetrahydropyrene core against oxidation and also that can potentially passivate the perovskite surfaceby coordination[32-36]. Furthermore, electron donating diphenylamine substitutents have been introduced in order to obtain optimal energy levels and solubility for solution-processable HTMs. Quart-*p*-phenylene **1** was investigated as a HTM in PSCs with a fluorine-doped tin oxide (FTO)/compact TiO_2/mesoporous TiO_2/$Cs_x(MA_{0.17}FA_{0.83})_{(100-x)}Pb(I_{0.83}Br_{0.17})_3$/**1**/Au configuration that show PCE, short circuit current (J_{SC}) open circuit voltage (V_{OC}) and fill factor (*FF*) values that are comparable to those of *spiro*-OMeTAD.

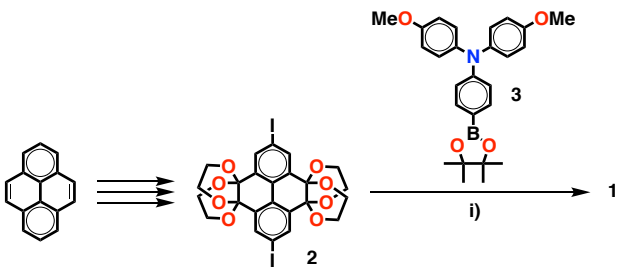

Scheme 1. Synthesis of **1**. Reaction conditions: *i)* K_2CO_3, $Pd(PPh_3)_4$, toluene, water, 90°C, 72 hours, 63%.

Quart-*p*-phenylene **1** is easily obtained in a gram-scale via Suzuki cross-coupling reaction between tetrahydropyrene **2** and triarylamine **3** in a good yield (63%). Precursors **2**[37-40] and **3**[41] were prepared from commercially available compounds in three and one steps, respectively. Quart-*p*-phenylene **1** showed a high stability under ambient conditions without any sign of decomposition after several months. Also, thermogravimetric analysis of **1** reveals a thermal stability up to *circa* 280 °C (Figure S4). Moreover, quart-*p*-phenylene **1** was soluble in common organic solvents (toluene, chlorobenzene, CH_2Cl_2, and $CHCl_3$).

The structure of quart-*p*-phenylene **1** was determined by ^{1}H-NMR, ^{13}C-NMR, HRMS and single crystal X-ray diffraction. Single crystals of **1** were obtained by slow vapor diffusion of EtOH into a solution of **1** in $CHCl_3$. The X-ray structures show that the two central rings on the tetrahydopyrene core are almost co-planar with a small torsion angle of 8° as an effect of the ketal substituents (Figure 2a). On the other hand, the torsion angle of the more external phenyl rings of the quart-*p*-phenylene core with the tetrahydropyrene reside is substantially higher (24°) as an effect of the free rotation. The distance of the central C-C bond between the phenyl rings of the tetrahydropyrene core was 1.468 Å, in agreement with the bond distance observed in tetrahydropyrene (1.470 Å)[42] for the same bond, which is slightly larger than that in pyrene (1.422 Å).

The optical properties of **1** were investigated in solution. Figure 2b shows the UV-Vis absorption and the normalized photoluminescence spectra of **1** in CH_2Cl_2. Quart-*p*-phenylene **1** absorbs light preferentially in the UV region of the electromagnetic spectrum, thus avoiding overlapping with the absorption of triple cation perovskite (*vide infra*). It shows two main absorption bands centered at 293 and 398 nm with large absorption coefficients, 47,716 and 68,695 L mol^{-1} cm^{-1}, respectively. The photoluminescence spectrum of **1** in CH_2Cl_2 (λ_{ex} = 370

nm) exhibited a single featureless emission band centered at 515 nm with a large Stokes shift of 117 nm.

To understand the nature of the main electronic transitions in **1**, time-dependent density functional theory (TD-DFT) was carried out in CH_2Cl_2 with the B3LYP Hamiltonian with a 6-311+g(2d,p) basis set on minimized geometries at the B3LYP-CH_2Cl_2-6-31(d,p) level (Supporting Information, Table S1). In addition, the natural transition orbitals were also computed to aid the visualization of the transitions (Figures S5 and S6). The calculations reproduced the difference in energy between both transitions (~ 1 eV). The experimental band at 383 nm is computed predominantly as the HOMO→LUMO transition (97%) with an oscillator strength of 1.482, whereas the experimental band at 293 nm is computed as the sum of two electronic transitions HOMO–2→LUMO (31%) and HOMO–1→LUMO+4 (53%), with an oscillator strength of 0.857.

The electrochemical properties of **1** were investigated by cyclic voltammetry in a CH_2Cl_2 solution using nBu$_4$NPF$_6$ (0.1 M) as the electrolyte (Figure 2c) in a three-electrode cell with a glassy carbon disk electrode as the working electrode, a Ag wire reference electrode and a Pt counter-electrode. The potential values are given *versus* the redox potential of the ferrocene/ferrocenium couple, which was used as an internal standard. Quart-*p*-phenylene **1** showed a reversible peak at $E_{1/2}$ = +0.23 V. No reduction processes were observed within the solvent-supported electrolyte window.

The optical energy gap (E_g = 2.78 eV) was estimated from the onset of the longest absorption band, and the HOMO level (or ionization potential) of **1** (E_{HOMO} = –4.97 eV) was estimated from the onset of the first oxidation process. The LUMO level (E_{LUMO} = –2.19 eV) was then estimated from the difference

between E_g and E_{HOMO}. Density Functional Theory calculations also provided information about the geometry, the energy levels and the electronic distribution of **1**. The experimental energy levels are in good agreement with the theoretical values (E_{HOMO} = –4.83 eV; E_{LUMO} = –1.74 eV) calculated at 6-311+g(2d,p) basis set with the B3LYP Hamiltonian. The electron density of the HOMO level of **1** is delocalized from the two external triphenylamine moieties across the biphenyl core (Figure 2d). The molecule shows large delocalization along the whole molecule due to its planarity and it is worth noting that the four methoxy groups also participate in the delocalization of the electron density. The experimental and calculated E_{HOMO} and E_{LUMO} values indicate that **1** is a very promising candidate to behave as a hole-transporting and electron-blocking material (Figure 2e).

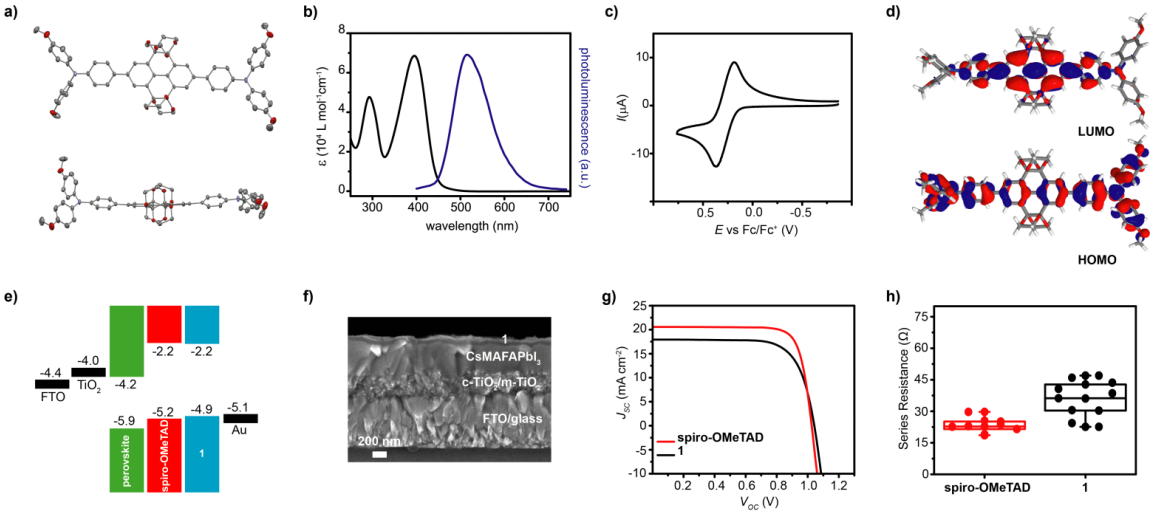

Figure 2. a) Two views for the X-ray crystal structure of **1**. b) UV–vis absorption (black) and photoluminescence (blue) spectra of **1** in CH_2Cl_2. c) Cyclic voltammogram of **1** in nBu_4NPF_6 in CH_2Cl_2 (0.1 mM). Potential *versus* the ferrocene/ferrocenium couple. d) Electronic density of the frontier orbitals of **1**. e) Energy levels (eV) of the different device components. f) FESEM cross section of a glass/FTO/c-TiO_2/mp-TiO_2/$Cs_x(MA_{0.17}FA_{0.83})_{(100-x)}Pb(I_{0.83}Br_{0.17})_3$/**1**/Au device. g) *J*–*V* curves of the best performing devices. h) Statistics of series resistance of working devices.

To test the behavior of quart-*p*-phenylene **1** as a HTM, we prepared regular mesoporous PSCs with the triple-cation perovskite[7] ($Cs_x(MA_{0.17}FA_{0.83})_{(100-x)}Pb(I_{0.83}Br_{0.17})_3$). The devices were fabricated using a configuration comprising layers of fluorine-doped tin oxide (FTO) glass/compact TiO_2/mesoporous TiO_2/perovskite/**1**/Au configuration. We also fabricated a set with *spiro*-OMeTAD instead of quart-*p*-phenylene **1**, as a reference. Both HTMs were doped with small amounts of (*bis*(trifluoromethylsulfonyl)imide lithium salt (LiTFSI) and 4-*tert*-butylpyridine (TBP).[43] A cross sectional FESEM micrograph of one of the devices shows clearly the heterostructure constituted by the different layers (Figure 2f). The observed thickness of the quart-*p*-phenylene **1** slab was around 70-90 nm. Notably, the HTM layer is compact and its thickness is uniform across the cell surface, which confirmed the high processability and suitability of this molecule for perovskite solar cells. The arithmetic roughness measured by AFM of a layer of quart-*p*-phenylene **1** directly on the ($Cs_x(MA_{0.17}FA_{0.83})_{(100-x)}Pb(I_{0.83}Br_{0.17})_3$) layer shows that **1** contributes to the smoothness of the cells (Figure S7 and S8).

We investigated quart-*p*-phenylene **1** deposited from chlorobenzene solutions with three different concentrations (15, 20 and 30 mM). The photovoltaic parameters of such solar devices were compared to those containing *spiro*-OMeTAD, illustrating the best performance for the ones fabricated from 30 mM solutions of quart-*p*-phenylene **1** (Figure S9). The *J*-*V* curves and the extracted cell parameters obtained for the best-performing cells using quart-*p*-phenylene **1** (30 mM in chlorobenzene) as HTMs (Figure 2g and Table 1) show PCE, J_{SC}, V_{OC} and *FF* values that are comparable to those of obtained for the *spiro*-OMeTAD reference cells. In particular, the average PCE (PCE_{av} = 12.8%) and the maximum PCE (PCE_{max} = 15.3%) observed for quart-*p*- phenylene **1** are

comparable to those values observed for *spiro*- OMeTAD (PCE_{ave} = 14.4% and PCE_{max} = 17.0%).

HTM	V_{OC}	J_{SC}	FF	PCE_{ave}	PCE_{max}
spiro-OMeTAD	1.009	20.6	78	14.4	17.0
1	1.042	17.9	73	12.8	15.3

Table 1. V_{OC} (V), J_{SC}, (mA cm^{-2}), FF (%) and PCE (%) of the devices.

The V_{OC} values of quart-*p*-phenylene **1** (V_{OC} = 1.042 V) are slightly higher than those measured for *spiro*-OMeTAD (V_{OC} = 1.009 V), while the J_{SC} values of quart-*p*-phenylene **1** (J_{SC} = 17.9 mA cm^{-2}) are slightly lower than those of *spiro*-OMeTAD (J_{SC} = 20.6 mA cm^{-2}). The FF of devices with **1** is lower, which can be rationalised in terms of the series resistance (R_s) observed in the different sets of devices (Figure 2h), which are obtained from the *J–V* curves measured under 1 sun irradiation in a backward scan. Both molecules showed satisfying R_s values, but in the case of quart-*p*-phenylene **1** are slightly higher, which account for the slightly smaller PCE values.

To conclude, we have described the synthesis and full characterization of a novel molecular hole transporting material based on a partially planarised quart-*p*-phenylene core. The optoelectronic (UV-vis absorption and photoluminescence), electrochemical, thermal and theoretical properties confirm that quart-*p*-phenylene **1** possesses a well aligned energy level arrangement and also an optimal stability and solubility to be implemented as a hole transporting and electron blocking material in PSCs. As a matter of fact, the characterization of regular $Cs_x(MA_{0.17}FA_{0.83})_{(100-x)}Pb(I_{0.83}Br_{0.17})_3$ PSC incorporating quart-*p*-phenylene **1** as a hole transporting material shows PCE, J_{SC}, V_{OC} and *FF* values

that are comparable to those obtained for the *spiro*-OMeTAD without any device optimization. We foresee that by further improvement of the deposition process and by controlling the number of rings and their planarization, the performance of oligo- and poly-*p*-phenylenes as HTM in PSCs can be further enhanced to rival with *spiro*-OMeTAD.

Notes and references

1. J.-P. Correa-Baena, M. Saliba, T. Buonassisi, M. Grätzel, A. Abate, W. Tress and A. Hagfeldt, *Science*, 2017, **358**, 739-744.
2. W. S. Yang, B.-W. Park, E. H. Jung, N. J. Jeon, Y. C. Kim, D. U. Lee, S. S. Shin, J. Seo, E. K. Kim, J. H. Noh and S. I. Seok, *Science*, 2017, **356**, 1376-1379.
3. C. Silvia, V. S. F. and D. J. Luis, *Angew. Chem. Int. Ed.*, 2015, **54**, 9757-9759.
4. N.-G. Park, M. Grätzel, T. Miyasaka, K. Zhu and K. Emery, *Nat. Energy*, 2016, **1**, 16152.
5. V. S. F., C. Silvia and D. J. Luis, *ChemSusChem*, 2015, **8**, 3012-3028.
6. Z. H. Li, M. S. Wong, Y. Tao and M. D'Iorio, *J. Org. Chem.*, 2004, **69**, 921-927.
7. M. Saliba, T. Matsui, J.-Y. Seo, K. Domanski, J.-P. Correa-Baena, M. K. Nazeeruddin, S. M. Zakeeruddin, W. Tress, A. Abate, A. Hagfeldt and M. Gratzel, *Energy Environ. Sci.*, 2016, **9**, 1989-1997.
8. W. Zhang, Y.-C. Wang, X. Li, C. Song, L. Wan, K. Usman and J. Fang, *Advanced Science*, 2018, **5**, 1800159.
9. T. T. Ngo, I. Suarez, G. Antonicelli, D. Cortizo-Lacalle, J. P. Martinez-Pastor, A. Mateo-Alonso and I. Mora-Sero, *Adv. Mater.*, 2017, **29**, 1604056.
10. V. D'Innocenzo, G. Grancini, M. J. P. Alcocer, A. R. S. Kandada, S. D. Stranks, M. M. Lee, G. Lanzani, H. J. Snaith and A. Petrozza, *Nat. Commun.*, 2014, **5**, 3586.
11. N. Liang, W. Jiang, J. Hou and Z. Wang, *Mater. Chem. Front.*, 2017, **1**, 1291-1303.
12. C. S. D., R. N. A., H. M. C. and N. Thuc-Quyen, *Adv. Energy Mater.*, 2017, **7**, 1602242.
13. G. Li, W.-H. Chang and Y. Yang, *Nat. Rev. Mater.*, 2017, **2**, 17043.
14. Y. Ma, Z. Kang and Q. Zheng, *J. Mater. Chem. A*, 2017, **5**, 1860-1872.

15. M. Pazoki, U. B. Cappel, E. M. J. Johansson, A. Hagfeldt and G. Boschloo, *Energy Environ. Sci.*, 2017, **10**, 672-709.

16. W. Ghann, H. Kang, T. Sheikh, S. Yadav, T. Chavez-Gil, F. Nesbitt and J. Uddin, *Scientific Reports*, 2017, **7**, 41470.

17. J.-P. Correa-Baena, A. Abate, M. Saliba, W. Tress, T. Jesper Jacobsson, M. Gratzel and A. Hagfeldt, *Energy Environ. Sci.*, 2017, **10**, 710-727.

18. X. Li, D. Bi, C. Yi, J.-D. Décoppet, J. Luo, S. M. Zakeeruddin, A. Hagfeldt and M. Grätzel, *Science*, 2016, **353**, 58-62.

19. D. P. McMeekin, G. Sadoughi, W. Rehman, G. E. Eperon, M. Saliba, M. T. Hörantner, A. Haghighirad, N. Sakai, L. Korte, B. Rech, M. B. Johnston, L. M. Herz and H. J. Snaith, *Science*, 2016, **351**, 151-155.

20. D. Bi, W. Tress, M. I. Dar, P. Gao, J. Luo, C. Renevier, K. Schenk, A. Abate, F. Giordano, J.-P. Correa Baena, J.-D. Decoppet, S. M. Zakeeruddin, M. K. Nazeeruddin, M. Grätzel and A. Hagfeldt, *Sci. Adv.*, 2016, **2**.

21. N. J. Jeon, J. H. Noh, W. S. Yang, Y. C. Kim, S. Ryu, J. Seo and S. I. Seok, *Nature*, 2015, **517**, 476.

22. L. Calió, S. Kazim, M. Grätzel and S. Ahmad, *Angew. Chem. Int. Ed.*, 2016, **55**, 14522-14545.

23. C. Rodríguez-Seco, L. Cabau, A. Vidal-Ferran and E. Palomares, *Acc. Chem. Res.*, 2018, **51**, 869-880.

24. M. F. L. De Volder, S. H. Tawfick, R. H. Baughman and A. J. Hart, *Science*, 2013, **339**, 535-539.

25. J. Grimme, M. Kreyenschmidt, F. Uckert, K. Müllen and U. Scherf, *Adv. Mater.*, 1995, **7**, 292-295.

26. M. Neophytou, J. Griffiths, J. Fraser, M. Kirkus, H. Chen, C. B. Nielsen and I. McCulloch, *J. Mat. Chem. C*, 2017, **5**, 4940-4945.

27. B. Xu, J. Zhang, Y. Hua, P. Liu, L. Wang, C. Ruan, Y. Li, G. Boschloo, E. M. J. Johansson, L. Kloo, A. Hagfeldt, A. K. Y. Jen and L. Sun, *Chem*, 2017, **2**, 676-687.

28. S. S. Reddy, K. Gunasekar, J. H. Heo, S. H. Im, C. S. Kim, D.-H. Kim, J. H. Moon, J. Y. Lee, M. Song and S.-H. Jin, *Adv. Mater.*, 2016, **28**, 686-693.

29. X. Li, X. Liu, X. Wang, L. Zhao, T. Jiu and J. Fang, *J. Mater. Chem. A*, 2015, **3**, 15024-15029.

30. H. Choi, S. Park, M.-S. Kang and J. Ko, *Chem. Commun.*, 2015, **51**, 15506-15509.

31. M. S. Kang, S. D. Sung, I. T. Choi, H. Kim, M. Hong, J. Kim, W. I. Lee and H. K. Kim, *ACS Applied Materials & Interfaces*, 2015, **7**, 22213-22217.

32. J. Cao, Y.-M. Liu, X. Jing, J. Yin, J. Li, B. Xu, Y.-Z. Tan and N. Zheng, *J. Am. Chem. Soc.*, 2015, **137**, 10914-10917.

33. D. W. de Quilettes, S. M. Vorpahl, S. D. Stranks, H. Nagaoka, G. E. Eperon, M. E. Ziffer, H. J. Snaith and D. S. Ginger, *Science*, 2015, **348**, 683-686.

34. Y.-H. Kim, H. Cho, J. H. Heo, T.-S. Kim, N. Myoung, C.-L. Lee, S. H. Im and T.-W. Lee, *Adv. Mater.*, 2015, **27**, 1248-1254.

35. C. Huang, W. Fu, C.-Z. Li, Z. Zhang, W. Qiu, M. Shi, P. Heremans, A. K. Y. Jen and H. Chen, *J. Am. Chem. Soc.*, 2016, **138**, 2528-2531.

36. H. Sung, N. Ahn, M. S. Jang, J.-K. Lee, H. Yoon, N.-G. Park and M. Choi, *Adv. Energy Mater.*, 2016, **6**, 1501873.

37. S. More, R. Bhosale, S. Choudhary and A. Mateo-Alonso, *Org. Lett.*, 2012, **14**, 4170-4173.

38. R. Garcia, M. Melle-Franco and A. Mateo-Alonso, *Chem. Commun.*, 2015, **51**, 8037-8040.

39. R. García, S. More, M. Melle-Franco and A. Mateo-Alonso, *Org. Lett.*, 2014, **16**, 6096-6099.

40. D. Cortizo-Lacalle, J. P. Mora-Fuentes, K. Strutyński, A. Saeki, M. Melle-Franco and A. Mateo-Alonso, *Angew. Chem. Int. Ed.*, 2018, **57**, 703-708.

41. K. Rakstys, A. Abate, M. I. Dar, P. Gao, V. Jankauskas, G. Jacopin, E. Kamarauskas, S. Kazim, S. Ahmad, M. Grätzel and M. K. Nazeeruddin, *J. Am. Chem. Soc.*, 2015, **137**, 16172-16178.

42. B. R. Kaafarani, A. a. O. El-Ballouli, R. Trattnig, A. Fonari, S. Sax, B. Wex, C. Risko, R. S. Khnayzer, S. Barlow, D. Patra, T. V. Timofeeva, E. J. W. List, J.-L. Bredas and S. R. Marder, *J. Mat. Chem. C*, 2013, **1**, 1638-1650.

43. E. J. Juarez-Perez, M. R. Leyden, S. Wang, L. K. Ono, Z. Hawash and Y. Qi, *Chem. Mater.*, 2016, **28**, 5702-5709.